Journal of The Electrochemical Society, **147** (12) 4645-4651 (2000)
S0013-4651(00)02-111-X CCC: $7.00 © The Electrochemical Society, Inc.

Microstructural Investigation of Ni/Au Ohmic Contact on p-Type GaN

Jong Kyu Kim,[a] Jung Ho Je,[a] Jong-Lam Lee,[a,z] Yong Jo Park,[b] and Byung-Teak Lee[c]

[a]*Department of Materials Science and Engineering, Pohang University of Science and Technology, Pohang 790-784, Korea*
[b]*Photonics Laboratory, Samsung Advanced Institute of Technology, Suwon 440-600, Korea*
[c]*Department of Metallurgical Engineering, Chonnam National University, Kwangju 500-757, Korea*

Microstructural changes in Ni/Au contacts to p-type GaN as a function of annealing temperature were investigated using X-ray diffraction, field emission scanning electron microscopy, and cross-sectional transmission electron microscopy combined with energy dispersive spectroscopy. The results obtained were used to interpret the electrical properties of Ni/Au ohmic contacts to p-type GaN. The contact resistivity decreased from 1.4×10^{-2} to $6.1 \times 10^{-4}\ \Omega\ cm^2$ after annealing at 600°C. The reduction in contact resistivity resulted from the dissolution of Ga atoms into the Au-Ni solid solution produced during annealing. Au atoms diffused to the GaN substrate through grain boundaries and reacted with Ni atoms at the grain boundaries of Ni, producing an Au-Ni solid solution. This resulted in the evolution of microstructure with island-shaped Ni grains surrounded by the Au-Ni solid solution. At this stage, Ga atoms outdiffused from the GaN substrate and dissolved into the Au-Ni solid solution, leading to the generation of Ga vacancies below the contact. Thus, the net concentration of holes below the contact increased, and so the contact resistivity was reduced. When the sample was annealed at 800°C, the Au layer completely reacted with the Ni layer, uniformly producing an Au-Ni solid solution containing Au-Ga and Ni-Ga compounds. Simultaneously, N atoms reacted with Ni, and produced cubic Ni_4N in the vicinity of the metal/GaN interface. Consequently, N vacancies, acting as donors in GaN, were generated below the contact, leading to an increase of contact resistivity to $4.0 \times 10^{-2}\ \Omega\ cm^2$.
© 2000 The Electrochemical Society. S0013-4651(00)02-111-X. All rights reserved.

Manuscript submitted February 28, 2000; revised manuscript received August 29, 2000.

The III-V nitride semiconductors, especially GaN, have received considerable attention for optoelectronic devices in blue and ultraviolet wavelengths as well as for its potential for high-temperature and high-power electronic devices.[1-3] In developing such devices, it is essential to develop thermally stable and low resistance ohmic contacts on both n- and p-type GaN in order to enhance their performance. For the ohmic contacts on n-type GaN, many investigations have been carried out. Ti- and/or Al-based metallization schemes were the most widely used ohmic contacts to n-type GaN. Related investigations proposed that the formation of TiN, AlN, and Al-Ti intermetallic compounds were attributed to such low contact resistance ranging between 10^{-5} and $10^{-7}\ \Omega\ cm^2$.[4-7] Recently, W- and Cr-based ohmic contacts to n-type GaN were found to enhance the long-term thermal stability.[8,9] However, it is difficult to obtain such low contact resistivities on p-type GaN because of the low hole concentrations in p-type GaN and high Schottky barrier height at the interface of metal with p-type GaN.[3] In fact, one of the main obstacles in realizing the continuous wave operation of GaN-based laser diodes (LDs) was the high contact resistance on p-type GaN.

Many attempts have been conducted to reduce the contact resistivity on p-type GaN. A number of metals with high work function such as Au, Ni, Pt, and Pd were intensively studied in an attempt to reduce the contact resistivity by lowering the Schottky barrier height at the metal/p-type GaN interface. Sheu *et al.*[10] investigated high-transparency Ni/Au ohmic contacts on p-type GaN with a specific contact resistivity of $1.7 \times 10^{-2}\ \Omega\ cm^2$ after annealing at 450°C. Jang *et al.*[11] reported Pt/Ni/Au contacts on p-type GaN ($3 \times 10^{17}\ cm^{-3}$) with $5.1 \times 10^{-4}\ \Omega\ cm^2$ after annealing at 350°C. The low contact resistivity of $3 \times 10^{-5}\ \Omega\ cm^2$ was obtained using Ta/Ti contact on p-type GaN ($7 \times 10^{17}\ cm^{-3}$).[12] A specific contact resistivity below $1.0 \times 10^{-4}\ \Omega\ cm^2$ was obtained by oxidizing Ni/Au contact on p-type GaN.[13] The low resistance ohmic contact was interpreted to be related to the formation of NiO. Lee *et al.*[14] investigated the effect of surface treatments prior to Pt deposition on contact resistivity. Contact resistivity was decreased from 5.1×10^{-2} to $2.5 \times 10^{-5}\ \Omega\ cm^2$ by the surface treatment using $(NH_4)_2S_x$ solution. Interfacial reactions between contact metal and p-type GaN with annealing also have been studied.[15-18] Trexler *et al.*[15] investigated the interfacial reactions of Ni/Au, Pd/Au, and Cr/Au contacts on p-GaN with annealing by Auger electron spectroscopy (AES) and current-voltage (*I-V*) characteristics. Rutherford back scattering spectroscopy (RBS) and X-ray diffraction (XRD) were also applied to find the interfacial reactions of Ni/Au contacts on p-type GaN.[16] The *I-V* curve became linear as the alloying temperature increased to 700°C because of the formation of Ga-Ni and Ga-Au compounds at the metal/GaN interface. Venugopalan *et al.*[17] reported the interfacial reactions of Ni and GaN at temperatures from 400 to 900°C in various atmospheres and estimated their results with the thermodynamics of the Ni-Ga-N system.

The electrical properties of metal contacts on semiconductor are largely affected by the interfacial reactions between the contact metal and the semiconductor during annealing, via production of point defects below the contact, which act as donors or acceptors at the subsurface of the semiconductor. In GaN, Ga vacancies, V_{Ga}s, are known to be triply charged acceptors,[18] acting a role to compensate electrons. Therefore, it is possible to increase the net concentration of holes below the contact, if V_{Ga}s, are produced at the subsurface of p-type GaN through the interfacial reactions, leading to the decrease of contact resistivity. On the contrary, the production of V_N results in the increase of contact resistivity. The Ni/Au is commonly used as ohmic contacts on p-type GaN films for light emitting diodes (LEDs) and LDs.[1,2] However, the interfacial reactions of Ni/Au contacts on p-type GaN have not yet been systematically studied in conjunction with the electrical properties of the contact, although many studies have been conducted as stated above.

In the present study, we investigated the interfacial reactions and microstructural changes of the Ni/Au ohmic contacts on p-type GaN during annealing. XRD was employed to identify the phases produced during annealing. Microstructural changes were studied using cross-sectional transmission electron microscopy (TEM) equipped with energy dispersive spectroscopy (EDS). The surface morphology of Au/Ni/GaN after annealing was examined by field emission scanning electron microscopy (SEM). From these results, the effects of interfacial reactions and the resultant microstructural changes of Ni/Au contacts on p-type GaN on the electrical properties of the contact are discussed.

Experimental

GaN films used were grown by metallorganic chemical vapor deposition (MOCVD) on *c* plane sapphire substrate. An undoped GaN layer with a thickness of 1 μm was grown, followed by the growth of 1 μm thick p-type GaN doped with Mg. Electrical activation of the grown samples was carried out at 800°C for 4 min by

[z] E-mail: jllee@postech.ac.kr

S0013-4651(00)02-111-X CCC: $7.00 © The Electrochemical Society, Inc.

rapid thermal annealing (RTA) under N_2 atmosphere. The net concentration of holes in the film was determined to be 2.9×10^{17} cm^{-3} by Hall measurements.

An active region for the evaluation of contact resistivity was defined by chemically assisted ion beam etching using Cl_2, followed by dipping the samples into a HCl:HNO_3 (3:1) solution to remove surface oxides formed on the p-type GaN.[14] Then, the sample was rinsed for 1 min with deionized water and dried with N_2 gas. 100 μm long and 200 μm wide transmission line method (TLM) test structures were patterned by photoresist. Ni(200 Å) and Au(500 Å) were deposited in sequence on the p-type GaN by an electron beam evaporator. The vacuum condition of the evaporator was maintained lower than 3×10^{-7} Torr during the deposition of the metal layers. After the metal deposition, the photoresist was lifted off. The TLM test structures were annealed for 30 s in the temperature range of 500-800°C by RTA under atmospheric pressure of N_2.

XRD with Cu Kα radiation was employed to identify the phase formed by the interfacial reactions of Ni/Au contacts on p-type GaN during annealing. The change of surface morphology of Au/Ni/GaN after annealing was examined by field emission SEM at an acceleration voltage of 15 kV, and elemental distribution was obtained by EDS of the individual regions. Microstructural and compositional analyses with annealing temperature were performed using a JEOL system (200 kV) equipped with a high resolution pole piece and ultrathin window X-ray detectors for the microdiffusion and EDS analysis.

Results

Electrical characteristics.—Figure 1 shows current-voltage (*I-V*) curves of the Ni/Au contacts on p-type GaN with annealing temperature measured between the TLM pads with an interspacing of 5 μm. In the as-deposited state, the *I-V* curve is nonlinear, but became linear over the whole range of voltages after annealing at 600°C. The *I-V* curves deteriorated as the annealing temperature increases to 800°C. The contact resistance (R_c) in the unit of ohms per millimeter and the sheet resistance (R_s) in the unit of Ω/□ were determined from the intercept of the y axis and the slope of resistances of 0 V with the interspacings of the TLM pads. The specific contact resistivity (ρ_c) was calculated by $\rho_c = R_c^2/R_s$, and the values determined are summarized in Table I and plotted in Fig. 2. A U-shaped dependence of contact resistivity on the annealing temperature was obtained. The contact resistivity decreased from 1.4×10^{-2} to 6.1×10^{-4} Ω cm^2 after annealing at 600°C. The lowest contact resistivity obtained was 3.6×10^{-4} Ω cm^2. A further increase of annealing temperature to 800°C resulted in the increase of contact resistivity to 4.0×10^{-2} Ω cm^2.

Table I. Contact resistivities of the Ni/Au contacts on p-type GaN as a function of annealing temperature.

Annealing temperature (°C)	Contact resistivity (Ω cm^2)
As-deposited	1.4×10^{-2}
500	3.2×10^{-3}
600	6.1×10^{-4}
700	1.3×10^{-3}
800	4.0×10^{-2}

Surface morphology and interfacial reaction.—Figure 3 shows the field emission SEM images of the Ni/Au contact on p-type GaN with annealing temperature. Surface morphology was not significantly changed up to 600°C, as shown in Fig. 3a and b. The metal films, however, began to form islands at 800°C, exposing the underlying GaN in some regions. The chemical compositions of the exposed region, marked as "1" in Fig. 3c were examined by EDS. Only Ga and N peaks were detected a shown in Fig. 4a, and their atomic percents correspond to 50.5 and 49.5%, respectively. In the island, marked as "2" in Fig. 3c, Au and Ni peaks were observed as well as Ga and N peaks, as shown in Fig. 4b. Results in Fig. 3 and 4 imply that most of metallic layers, Au and Ni, reacted with each other at 800°C.

Figure 5 shows XRD patterns of the Ni/Au contacts on p-type GaN as a function of annealing temperature. In the as-deposited state, XRD peaks corresponding to GaN, sapphire, Ni, and Au were observed. The Ni layer was grown on the p-type GaN with the preferred orientation, Ni(111)//GaN(0002), and Au overlayer was deposited epitaxially on the Ni layer with the preferred orientation, Au(111)//Ni(111). These results are consistent with previously reported results.[19] No reaction between the Ni and p-type GaN was observed. The XRD patterns of the samples annealed at 500 to 600°C reveal no difference from the as-deposited XRD patterns, except for the shift of Au peaks to higher angles with annealing temperature. In order to observe the change of Au and Ni peaks with annealing temperature in detail, the narrow range of diffraction

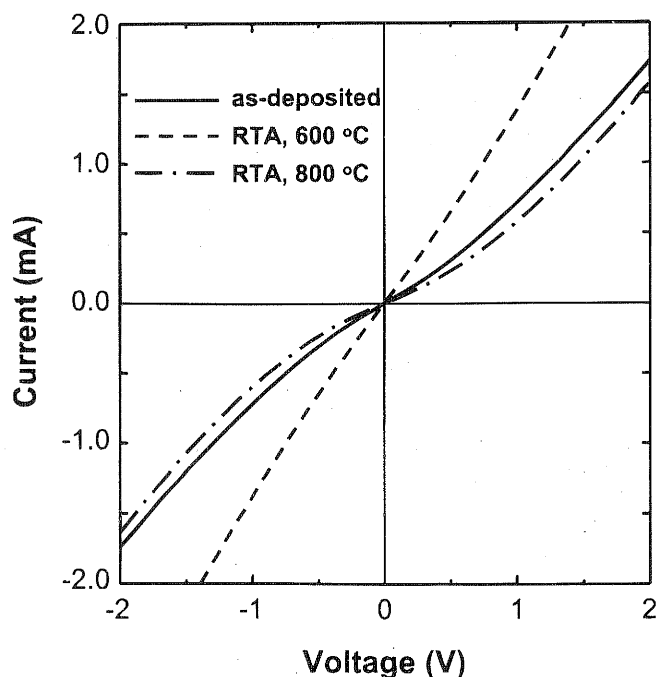

Figure 1. *I-V* curves of the Ni/Au contacts on p-type GaN with annealing temperature, measured between the TLM pads with a interspacing of 5 μm.

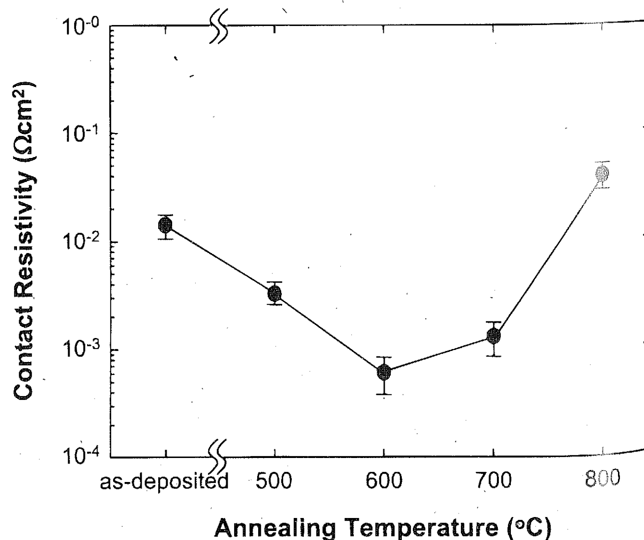

Figure 2. Change of the specific contact resistivity of the Ni/Au contacts on p-type GaN as a function of annealing temperature.

Journal of The Electrochemical Society, 147 (12) 4645-4651 (2000)
S0013-4651(00)02-111-X CCC: $7.00 © The Electrochemical Society, Inc.

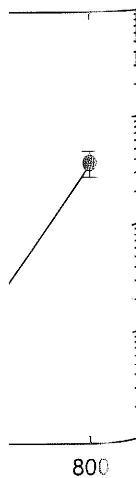

angles in Fig. 5a is enlarged as shown in Fig. 5b. The peak corresponding to Ni(111) does not change up to 600°C indicating no alteration in the lattice parameter of Ni. The lattice parameter of Ni measured to be 3.52 ± 0.01 Å, which value compared favorably with the lattice parameter of pure Ni (3.5240 Å),[20] and did not change up to 600°C. On the other hand, the peaks corresponding to Au(111) and Au(222) shift to higher angles with the increase of annealing temperature. This means that the distances between adjacent (111) planes, d_{111} and d_{222}, decrease with annealing temperature, namely, the decrease of lattice parameter. In order to observe the change of the lattice constant of Au in detail, the difference of d_{hkl} in Au, Δd_{hkl}, was calculated by subtracting the values of d_{hkl} in the annealed samples from that in the as-deposited one, which is summarized in

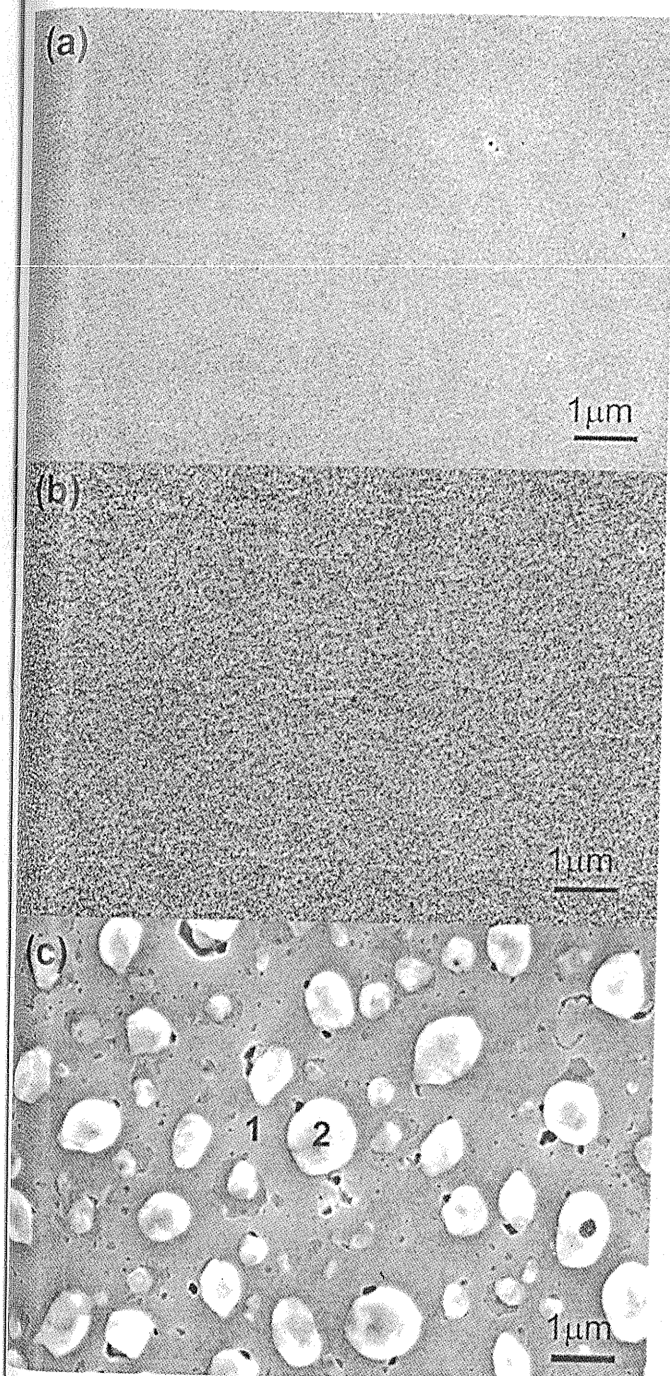

Figure 3. Field emission SEM images of Ni(200 Å)/Au(500 Å) contacts on p-type GaN; (a) in as-deposited state, (b) after annealing at 600°C, and (c) after annealing at 800°C.

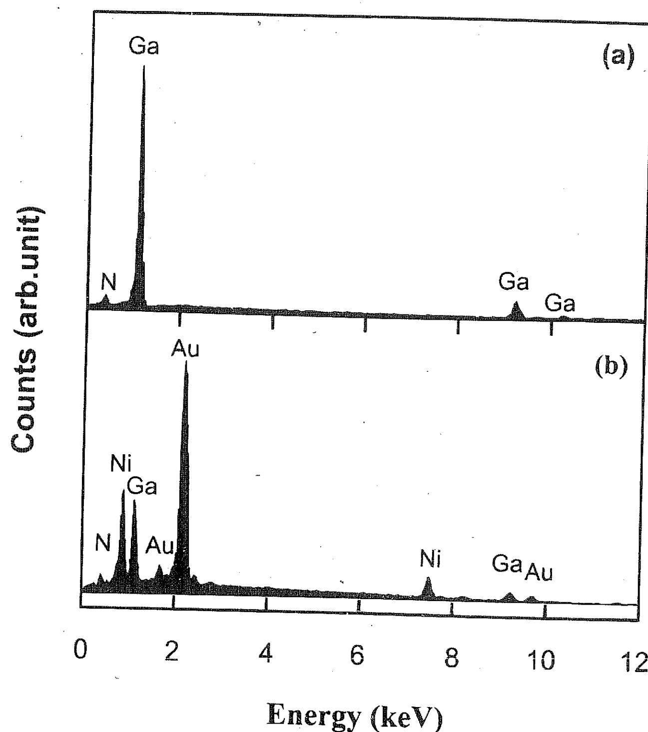

Figure 4. EDS analysis of the Ni/Au contact on p-type GaN; (a) EDS spectrum from the exposed region, marked as "1" in Fig. 3c, and (b) EDS spectrum from the metal island, marked as "2" in Fig. 3c.

Table II. Note that the changes of Δd_{111} are twice against those of Δd_{222} at each temperature. This suggests that the shift of Au peaks results from the change of lattice parameter of Au, due to the dissolution of impurity atoms in Au matrix. After annealing at 800°C, peaks corresponding Au-Ga compounds (Au_7Ga and $Au_{0.87}Ga_{0.13}$), Ni compounds (Ga_3Ni_5 and Ga_3Ni_2), and Ni_4N were observed. The inset of Fig. 5a shows the enlarged XRD pattern ranging from 80° to 100°. At a glance, three more peaks were included in the lower angle side than the sapphire peak (90.80°), but we could not fit the spectrum into three Gaussian and/or Lorentzian peaks. This implies that an additional peak was superimposed in the XRD pattern. We could separate the spectrum into four peaks, and the fourth peak was nearly in accordance with Ni_4N (311).

Microstructural analysis.—Figure 6a shows the cross-sectional TEM micrograph of the Ni/Au contacts on p-type GaN annealed at 600°C. A part of the ohmic metal penetrates into GaN substrate, as shown in the left rectangle of the micrograph, but some region maintains the original interface, as shown in the right rectangle in Fig. 6a. To investigate the interfacial reactions between Au, Ni, and GaN in detail, TEM with high magnification and EDS analyses were performed. Figures 6b and c are TEM micrographs with higher magnification on both regions marked in Fig. 6a. Ohmic metals penetrated deep by 150-250 Å below the original interface of Ni/GaN, as shown in Fig. 6. This indicates that the GaN substrate reacted with the metal layers during annealing at 600°C. Figure 6c shows the region maintaining a sharp interface between the metal and GaN. In both the regions, discrete grain islands with white image, marked as "1" in Fig. 6b and c, are distributed in the metallic layer on GaN. The chemical compositions of the white grain islands were analyzed using EDS, and the resultant spectrum is shown in Fig. 7a. This spectrum indicates that the island primarily consists of Ni with a small amount of Au and Ga. This implies that the white image corresponds to unreacted Ni grain. Figure 7b shows the EDS spectrum of the region with darker contrast, marked at "2" in Fig. 6b and c. In this region, the peaks corresponding to Au, Ni, and Ga are observed, The peak intensity of Au is higher than Ni. Considering the phase dia-

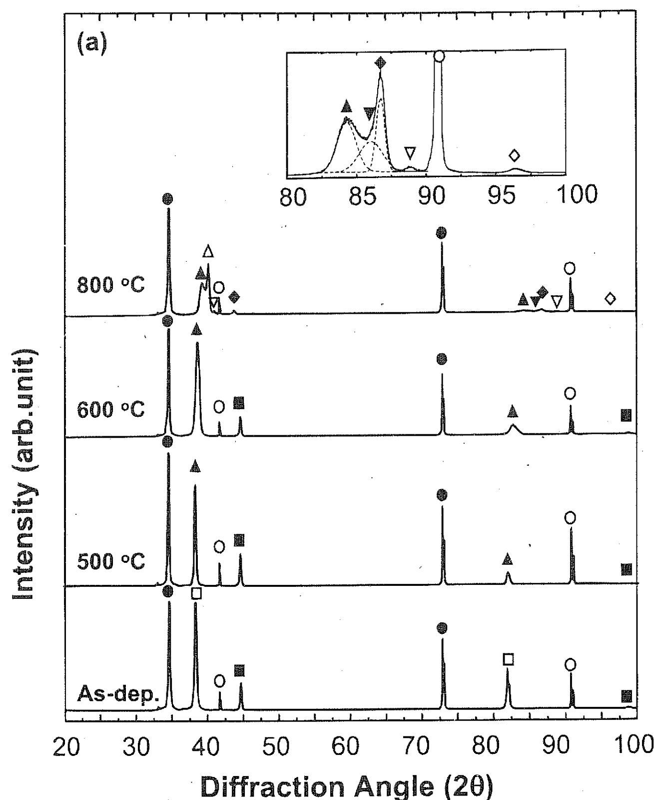

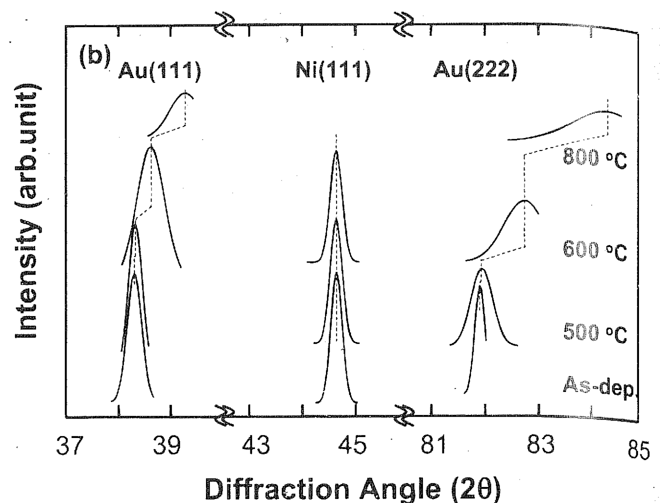

Figure 5. Change of XRD patterns of Ni/Au on p-type GaN with annealing temperature (a) (●) GaN, (○) Al_2O_3, (■) Ni, (▼) Ni_4N, (□) Au, (◆) Ga_3Ni_5, (▽) $Au_{0.87}Ga_{0.13}$, (△) Au_7Ga, (◇) Ga_3Ni_2, (▲) Au-Ga solid solution. The inset shows the XRD pattern from 80 to 100° to show the existence of Ga_3Ni_2. (b) Shift of XRD patterns of Au and Ni peaks.

gram of Au-Ni[21] and XRD results in Fig. 5, the dark region in Fig. 6b and c is related to Au-Ni solid solution containing Ga atoms. Note that the amount of Ga dissolved in the Au-Ni solid solution (dark image) is comparably larger than in the Ni grain (white image).

Figure 8a shows the TEM micrograph of the Ni/Au contacts annealed at 800°C. A part of the metal layer agglomerated and penetrated deep into GaN substrate. The GaN substrate was partly exposed, as marked by an arrow in Fig. 8a. A selected region, marked with rectangle in Fig. 8a, was magnified as shown in Fig. 8b. The white grains of small size (~50 Å), marked by an arrow in Fig. 8b, were mainly distributed in the vicinity of the penetrated metal/GaN interface.

This small white grain was analyzed through the selected area electron diffraction (SAED), and its resultant pattern and schematic illustration are displayed, respectively, in Fig. 9a and b. The incident electron beam was parallel to the direction of <001> zone axes of Au. The solid circles in Fig. 9b exactly coincide with the <001> pattern of cubic Ni_4N. In the phase diagram of the Au-Ni system, there is a large miscibility gap.[21] Thus, the Au-Ni solid solution might be separated into Au-rich and Ni-rich phases during cooling. The satellite spots drawn with the open circles and diamonds were overlapped with the Ni_4N pattern, which show fourfold symmetry. The lattice parameter calculated from the open circle was 4.065 Å, which is slightly smaller than that of Au (4.078 Å). The lattice parameters measured from the diamond pattern calculated to be 3.568 Å, slightly larger than that of Ni (3.524 Å). Therefore, we suggest that the satellite spots in Fig. 9a correspond to Au-rich and Ni-rich phases in the Au-Ni solid solution. The overlapping of the Au-rich and the Ni-rich phases into the Ni_4N diffraction pattern is due to the smaller size of Ni_4N (40~50 Å) grains than the electron beam size. Considering XRD results in Fig. 5, the dark region is composed of Au-Ga compounds, Au_7Ga and $Au_{0.87}Ga_{0.13}$, and Ni-Ga compounds, Ga_3Ni_5 and Ga_3Ni_2, as well as the Au-Ni solid solution.

Table II. Values of the distances between adjacent (*hkl*) planes, d_{hkl}, and the difference of d_{hkl}, calculated by subtracting the values of d_{hkl} in the annealed samples from that in the as-deposited one, Δd_{hkl}, as a function of annealing temperature.

	d_{111}	d_{222}	Δd_{111}	Δd_{222}
As-deposited	2.3474	1.1752	—	—
500°C	2.3463	1.1746	0.0011	0.0006
600°C	2.3284	1.1657	0.0190	0.0095
800°C	2.2917	1.1478	0.0557	0.0274

Discussion

Interfacial reactions and microstructure.—The microstructural change of the Ni/Au contact with annealing temperature, deduced from TEM analysis, are schematically illustrated in Fig. 10. In the as-deposited state, the original interface of Ni/Au contact on p-type GaN was abrupt and a number of grain boundaries existed because of the large lattice mismatch (~22%) between Ni(111) and the basal plane of GaN,[19] as displayed in Fig. 10a. When Ni/Au contacts were annealed at 600°C, Au atoms diffuse to GaN and react with both the Ni layer and GaN substrate. During annealing for 30 s at 600°C, the diffusion length of Au atoms through the lattice site of Ni is only 5.7 Å.[22] This suggests that Au atoms diffused through grain boundaries and reacted with Ni ones, producing Au-Ni solid solution. Formation of the Au-Ni solid solution at the grain boundary of Ni film results in the evolution of discrete array of Ni, as shown in Fig. 10b. During the process, Ga atoms outdiffused from the GaN substrate and dissolved into the Au-Ni solid solution.

When the sample was annealed at 800°C, the Au-Ni solid solution with the dark image penetrated deeper into GaN, exposing the underlying GaN in some regions, as shown in Fig. 10c. The diffusion length of the Au atom through the lattice site of Ni for 30 s at 800°C is about 190 Å when the sample was annealed for 30 s at 800°C.[22] Thus, the 200 Å thick Ni films could be completely reacted with Au. During the reaction, Au-Ga compounds, Au_7Ga and $Au_{0.87}Ga_{0.13}$ and Ni-Ga compounds, Ga_3Ni_5 and Ga_3Ni_2, as well as the Au-Ni solid solution were produced. The free N atoms below the contact outdiffused and reacted with unreacted Ni, producing Ni_4N, as well.

S0013-4651(00)02-111-X CCC: $7.00 © The Electrochemical Society, Inc.

as the generation of N vacancies, V_N. Consequently, both V_{Ga} and V_N were produced below the Ni/Au contact at 800°C.

One can argue that the formation of Ni_4N originated from the annealing ambient of N_2. It was reported that nitrogen is found to be insoluble in solid or liquid Ni and Au up to 1300°C.[23] For the dissolution of nitrogen gas into Ni, $1/2N_2(g) \rightarrow N\ [Ni]$, the standard Gibbs energy for the dissolution reaction is given by $\Delta G^\circ = +69100 + 6.0\ T$.[24] The Gibbs energy change for the reaction is positive inde-

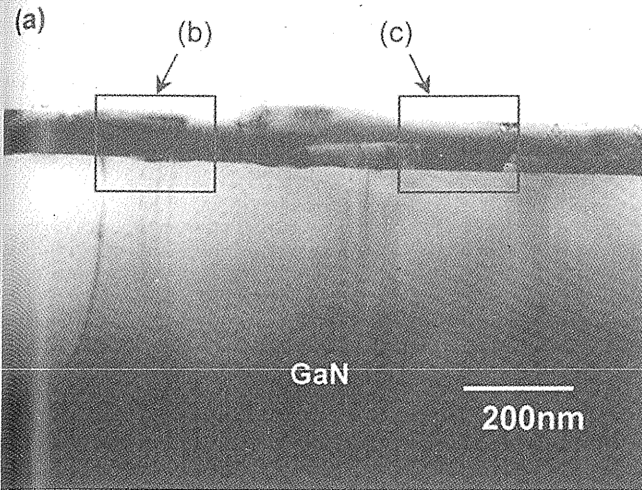

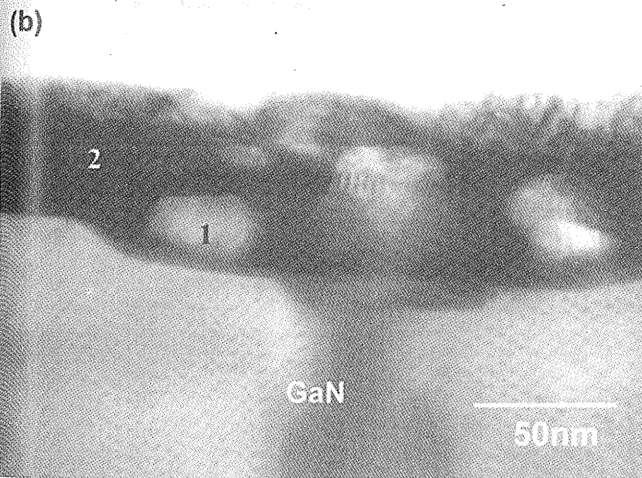

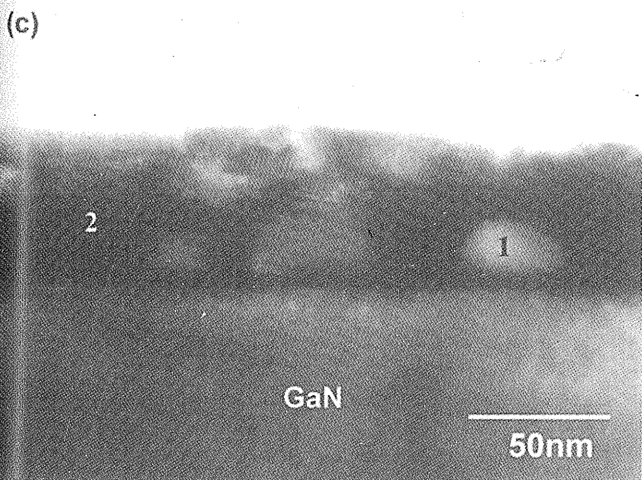

Figure 6. Cross-sectional TEM micrograph of Au/Ni/GaN annealed at 600°C; (a) with low magnification and (b) and (c) with high magnification.

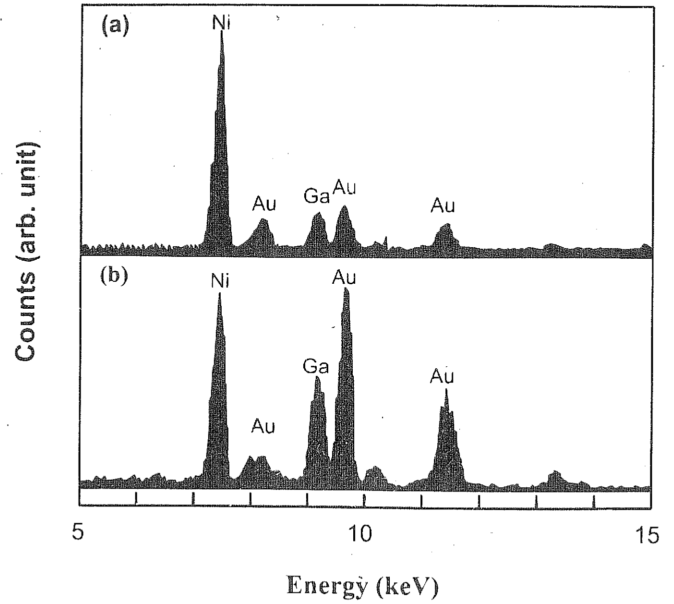

Figure 7. EDS analysis of the Ni/Au contact on p-type GaN annealed at 600°C; (a) in large grain islands with white image, marked at "1" in Fig. 6c and (b) in the dark image, marked as "2" in Fig. 6c.

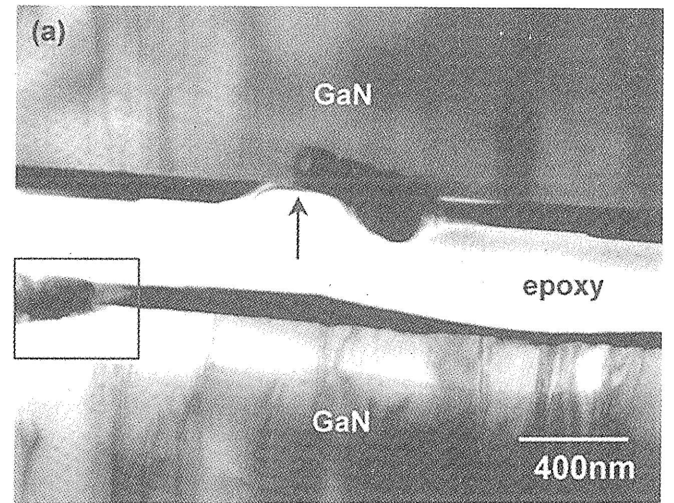

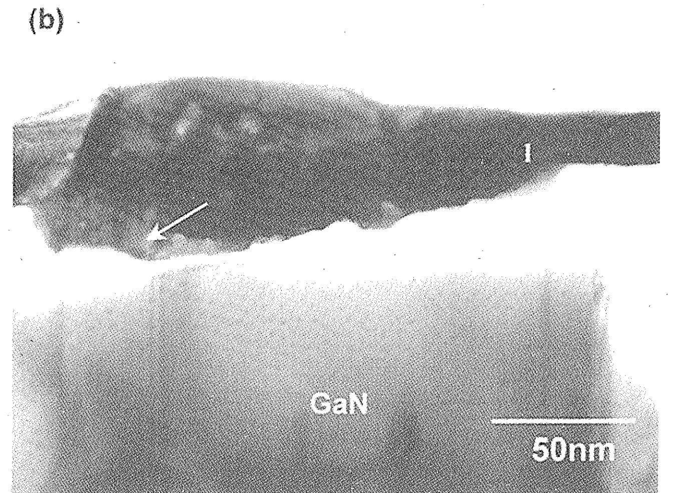

Figure 8. TEM micrograph of Au/Ni/GaN annealed at 800°C; (a) with low magnification, (b) with high magnification.

S0013-4651(00)02-111-X CCC: $7.00 © The Electrochemical Society, Inc.

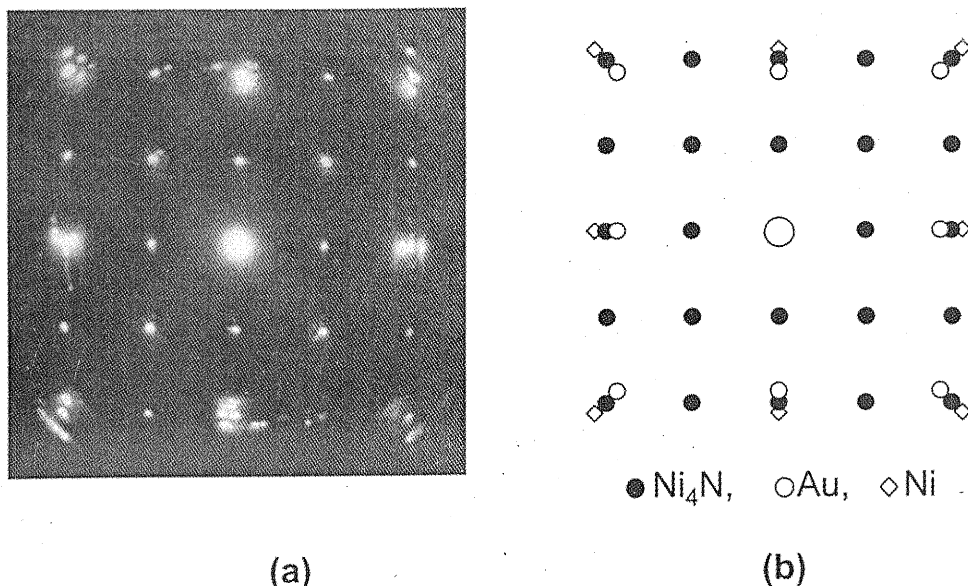

Figure 9. (a) SAED pattern of the small grains with white image, marked by an arrow in Fig. 8b, parallel to the direction of <001> zone axes of Au, and (b) its schematic illustration.

pendent of annealing temperature. This means that the nitrogen molecules in the annealing ambient could not be dissolved in Ni to form

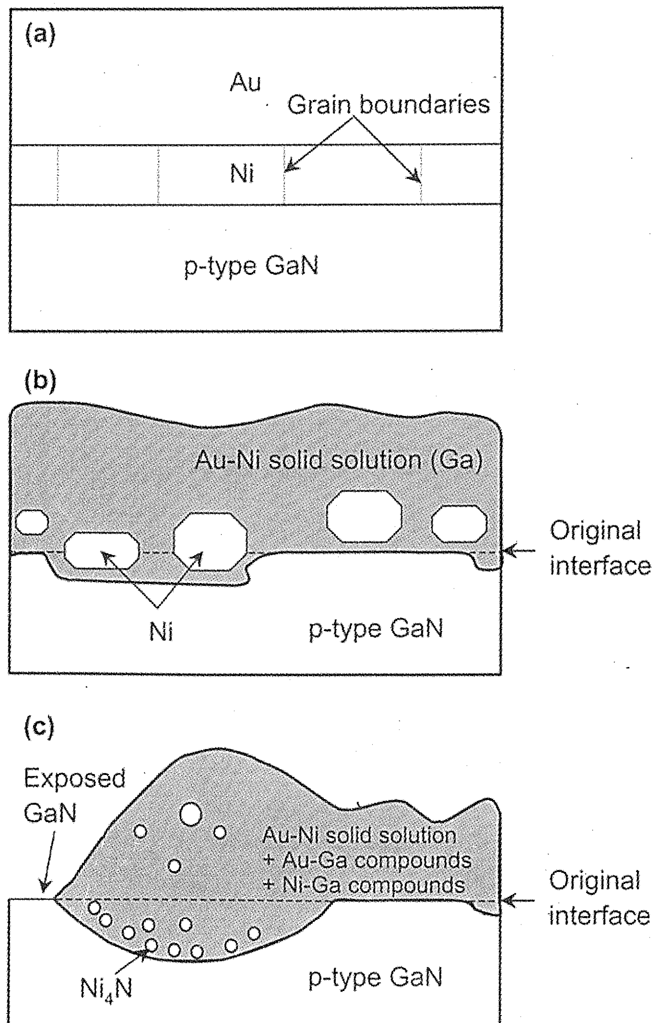

Figure 10. Schematic illustrations of the microstructure at the interface of Ni/Au contact on p-type GaN; (a) as-deposited state, (b) after annealing at 600°C and (c) after annealing at 800°C.

Ni_4N. Therefore, it is suggested that the Ni_4N phase in Fig. 8b originated from the interfacial reaction between metal film and GaN.

Correlation between electrical properties of contacts and microstructures.—The electrical properties of the Ni/Au contact on p-type GaN are discussed with the microstructural changes. Interfacial reactions between contact metal and GaN could produce point defects, which act as donors or acceptors at the subsurface of semiconductors. In GaN, Ga vacancies, V_{Ga}, are known to be triply charged acceptors,[18] acting to compensate electrons in n-type of GaN. Therefore, it is possible to increase net concentration of holes below the contact, if V_{Ga} are produced at the subsurface of p-type GaN through the interfacial reactions. When the sample is annealed at 600°C, Ga atoms outdiffused to the metal layer. In the XRD results, the values of Δd_{111} are changed nearly twice that of Δd_{222} at each temperature. Magnitude of Δd_{111} of Au in the Ni/Au contact on p-type GaN increases with annealing temperature, but no change of Δd of Ni was observed until the onset of Ni nitride formation. This suggests that the peak shift is due to the dissolution of Ga atoms in the solid solution as well as the formation of Au-Ni solid solution.

Comparing contact resistivities in Table I with interfacial reactions in Fig. 5, the decrease in contact resistivity at 600°C for the Ni/Au contact is closely related to the dissolution of Ga in Au-Ni solid solution, as displayed in Fig. 7b. The outdiffused Ga atoms lead to the generation of V_{Ga} at the subsurface of p-type GaN below the contact. Thus, electron compensating holes in p-type GaN are captured by V_{Ga}, leading to an increase in the net concentration of holes below the contact. Consequently, the depletion layer width below the contact and the effective Schottky barrier height for the transport of holes are simultaneously decreased, resulting in the reduction of contact resistivity. When the annealing temperature increases to 800°C, nickel nitride was found.

Conclusions

The contact resistivity of Ni/Au contacts on p-type GaN decreased from 1.4×10^{-2} to $6.1 \times 10^{-4}\ \Omega\ cm^2$ after annealing at 600°C, but increased to $4.0 \times 10^{-2}\ \Omega\ cm^2$ at 800°C. The reduction of contact resistivity at 600°C resulted from the formation of Au-Ni solid solution dissolving Ga atoms.

At 600°C, Au atoms diffused into the GaN substrate through grain boundaries and reacted with Ni ones in the grain boundaries of Ni, producing an Au-Ni solid solution. This results in the evolution of the microstructure with the island shape of Ni surrounded by the Au-Ni solid solution. At this stage, Ga atoms outdiffused from the GaN and dissolved into the Au-Ni solid solution because of the large solubility of Ga atoms in Au, leading to the generation of V_{Ga} below

S0013-4651(00)02-111-X CCC: $7.00 © The Electrochemical Society, Inc.

the contact. Thus, the net concentration of holes below the contact increased, resulting in the reduction of contact resistivity.

At 800°C, the Au layer completely reacted with the Ni layer, leading to the formation of the Au-Ni solid solution over the metal layer. The free N atoms reacted with Ni, leading to the formation of cubic Ni_4N in the vicinity of the metal/GaN interface. Consequently, V_N, acting as donors in GaN, lead to the increase of contact resistivity. Thus, N vacancies, V_N, acting as donors for electrons, are produced, resulting in the decrease of net concentration of holes. This causes the increases of the effective Schottky barrier height, leading to the increase of contact resistivity.

Acknowledgments

This work was supported in part by the Korea Institute of Science and Technology Evaluation and Planning through the NRL projects.

Korea Institute of Science and Technology Evaluation and Planning assisted in meeting the publication costs of this article.

References

1. S. Nakamura, M. Senoh, S. Nagahama, N. Iwasa, T. Matsushita, and T. Mukai, *Appl. Phys. Lett.*, **76**, 22 (2000).
2. S. Nakamura, M. Senoh, S. Nagahama, N. Iwasa, T. Yamada, T. Matsushita, H. Kiyoku, Y. Sugimoto, T. Kozaki, H. Umemoto, M. Sano, and K. Chocho, *Appl. Phys. Lett.*, **72**, 2014 (1998).
3. S. J. Pearton, J. C. Zolper, R. J. Shul, and F. Ren, *J. Appl. Phys.*, **86**, 1 (1999).
4. J. K. Sheu, Y. K. Su, G. C. Chi, M. J. Jou, C. C. Liu, C. M. Chang, W. C. Hung, J. S. Bow, and Y. C. Yu, *J. Vac. Sci. Technol. B*, **18**, 729 (2000).
5. L. L. Smith, R. F. Davis, R.-J. Liu, M. J. Kim, and R. W. Carpenter, *J. Mater. Res.*, **14**, 1032 (1999).
6. C.-T. Lee and H.-W. Kao, *Appl. Phys. Lett.*, **76**, 2364 (2000).
7. Q. Z. Liu and S. S. Lau, *Solid-State Electron.*, **42**, 677 (1998).
8. X. A. Cao, F. Ren, S. J. Pearton, A. Zeitouny, M. Eizenberg, C. R. Abernathy, J. Han, R. J. Shul, and J. R. Lothian, *J. Vac. Sci. Technol. A*, **17**, 1221 (1999).
9. N. A. Papanicolaou, A. Edwards, M. V. Rao, J. Mittereder, and W. T. Anderson, *J. Appl. Phys.*, **87**, 380 (2000).
10. J. K. Sheu, Y. K. Su, G. C. Chi, P. L. Koh, M. J. Jou, C. M. Chang, C. C. Liu, W. C. Hung, and K. Lin, *Appl. Phys. Lett.*, **74**, 2340 (1999).
11. J.-S. Jang, I.-S. Chang, H.-K. Kim, T.-Y. Seong, S. Lee, and S.-J. Park, *Appl. Phys. Lett.*, **74**, 70 (1999).
12. M. Suzuki, T. Kawakami, T. Arai, S. Kobayashi, Y. Koide, T. Umera, N. Shibata, and M. Murakami, *Appl. Phys. Lett.*, **74**, 275 (1999).
13. J.-K. Ho, C.-S. Jong, C. C. Chiu, C.-N. Huang, C.-Y. Chen, and K.-K. Shin, *Appl. Phys. Lett.*, **74**, 1275 (1999).
14. J.-L. Lee, J. K. Kim, J. W. Lee, Y. J. Park, and T. Kim, *Electrochem. Solid-State Lett.*, **3**, 53 (2000).
15. J. T. Trexler, S. J. Pearton, P. H. Holloway, M. G. Mier, K. R. Evans, and R. F. Karlicek, *Mater. Res. Soc. Symp. Proc.*, **449**, 1091 (1997).
16. J. K. Sheu, Y. K. Su, G. C. Chi, W. C. Chen, C. Y. Chen, C. N. Huang, J. M. Hong, Y. C. Yu, C. W. Wang, and E. K. Lin, *J. Appl. Phys.*, **83**, 3172 (1998).
17. H. S. Venugopalan, S. E. Mohney, B. P. Luther, S. D. Wolter, and J. M. Redwing, *J. Appl. Phys.*, **82**, 650 (1997).
18. J. Neugebauer and C. G. Van de Walle, *Appl. Phys. Lett.*, **69**, 503 (1996).
19. Q. Z. Liu, K. V. Smith, E. T. Yu, S. S. Lau, N. R. Perkins, and T. F. Kuech, *Mater. Res. Soc. Symp. Proc.*, **449**, 1079 (1997).
20. S. Y. Lee and P. Nash, in *Phase Diagrams of Binary Nickel Alloys*, P. Nash, Editor, p. 137, ASTM International, Materials Park, OH (1991).
21. H. Okamoto and T. B. Massalski, in *Phase Diagrams of Binary Gold Alloys*, T. B. Massalski, Editor, p. 196, ASTM International, Materials Park, OH (1987).
22. C. J. Smithells, in *Metals Reference Book*, 5th ed., C. J. Smithells, Editor, Butterworths, London (1976).
23. M. Hansen, *Constitution of Binary Alloys*, 2nd ed., pp. 217, 984, Butterworths, London (1978).
24. H. Okamoto and T. B. Massalski, in *Phase Diagrams of Binary Gold Alloys*, T. B. Massalski, Editor, p. 216, ASTM International, Materials Park, OH (1987).